

1 **PROBABILISTIC STUDY ON HYDRAULIC CONDUCTIVITY OF**
2 **CONCRETE AT MESO-SCALE**

3 Chun-Qing Li^{1,*}, Hassan Baji² and Shangtong Yang³

4 ¹Professor, School of Engineering, RMIT University, Melbourne, Australia,

5 *Corresponding Author Email: chungqing.li@rmit.edu.au

6 ²Lecturer, School of Engineering and Technology, Central Queensland University, Cairns,

7 Australia, Email: h.baji@cqu.edu.au

8 ³Lecturer, Department of Civil and Environmental Engineering, University of Strathclyde,

9 Glasgow, UK, Email: shangtong.yang@strath.ac.uk

10 **ABSTRACT**

11
12
13 Hydraulic conductivity of concrete can be used as a key indicator in assessment of service life of
14 concrete structures. In this paper, a probabilistic investigation on hydraulic conductivity of concrete
15 is conducted, allowing for variation in hydraulic properties of concrete constituents. Concrete is
16 modeled as a three-phase composite at meso-scale, consisting of mortar, aggregates and the
17 Interfacial Transition Zone (ITZ). A Finite Element (FE) method is developed to calculate the
18 hydraulic conductivity of concrete, which is then verified using available experimental results.
19 Based on a large pool of samples generated from Monte Carlo simulation, a conceptual model
20 relating hydraulic conductivity of concrete to aggregate volume fraction ratio and hydraulic
21 conductivity of mortar and the ITZ is proposed. It is shown from the probabilistic-based sensitivity
22 analysis that hydraulic conductivity and thickness of the ITZ are amongst the most influential
23 factors affecting the bulk hydraulic conductivity of concrete. It is also shown that for high aggregate
24 volume fraction ratios, due to increasing volume of the ITZ, the coefficient of variation of hydraulic
25 conductivity can be as high as 0.36.

26 **Keywords:** Concrete; Hydraulic Conductivity; Meso-scale; Probabilistic

INTRODUCTION

1
2
3
4
5
6
7
8
9
10
11
12
13
14
15
16
17
18
19
20
21
22
23
24
25
26

In most of the concrete deterioration processes, e.g., corrosion of reinforcing steel, water is either the principal cause of deterioration or the principal medium by which aggressive agents such as chloride or sulphate ions are transported into the concrete. It has been reported that water ingress is the main cause of deterioration in tunnel linings (ITA Working Group on Maintenance 1991; Russell and Gilmore 1997) leading to considerable cost of remediation and strengthening. Therefore, the long-term durability of concrete material is essentially related to its moisture transport properties. Service life of concrete structures, as a measure of their durability, can be directly quantified using moisture transport properties of concrete (Ho and Chirgwin 1996; Murata et al. 2004). Water ingress in concrete can be classified into two types: pressurized seepage flow through saturated concrete and the strongly nonlinear capillary-driven flow through unsaturated concrete. Water flow through unsaturated concrete follows the Fickian diffusion (Hall 1994; Leech et al. 2003), in which the hydraulic diffusivity coefficient is the most important moisture transport property. In this type of flow, the water penetration depth can be used as a service life measure (Lockington et al. 2002). On the other hand, flow of water in saturated media including concrete follows the Darcy's law with the hydraulic conductivity as the main water transport property. In order to make an adequately accurate service life prediction, it is vital that the water transport properties of concrete and factors influencing them are correctly characterized.

As concrete is a heterogeneous composite comprising of cement paste and randomly distributed fine and coarse aggregates, water transport properties of concrete significantly depend on its pore structure, e.g., the pore diameter and distribution, and the pore continuity and tortuosity, and to some extent micro cracking (Li et al. 2005). In porous media, transport properties are defined according to porosity, which is a function of water cement ratio and degree of hydration (Young and Hansen 1987). Relationships linking the diffusivity and conductivity to porosity can be found in the literature (Garboczi and Bentz 1996; Halamickova et al. 1995). The Interfacial Transition Zone (ITZ), which is formed due to the presence of aggregates, is highly porous. It is believed that the

1 porosity and as such conductivity of the ITZ is considerably higher than that of the surrounding
2 matrix, i.e., the cement paste (Winslow et al. 1994), which can have a considerable effect on the
3 transport performance of concrete. Nonetheless, there is little information about size and porosity of
4 this zone (Zheng et al. 2005). A wide range of 10 μm (3.94×10^{-7} in)-300 μm (1.18×10^{-5} in) has been
5 reported for the size of ITZ (Nemati and Gardoni 2005; Ollivier et al. 1995). Breton et al. (1992)
6 have reported that the effective diffusivity of this zone is 6-12 greater than that of bulk cement
7 paste. Shane et al. (2000) reported that the mortar conductivity is predicted to be about 10 times
8 higher than that of a bulk mortar. It has also been shown that porosity of this zone is highest at the
9 contact with aggregates and decreases with distance from aggregates (Bentz and Garboczi 1991;
10 Scrivener et al. 2004; Wu et al. 2016).

11 On the other hand, since most aggregates used in concrete are dense compared to the cement paste,
12 it is usually assumed that they have zero conductivity or diffusivity (Li et al. 2016; Wang and Ueda
13 2013). The inclusion of these nonconductive aggregates has an inverse effect on the diffusivity and
14 conductivity of the concrete composite. Various expressions relating the conductivity and
15 diffusivity of composites to volume fraction of aggregates are available in the literature (Hall et al.
16 1993; Hasselman and Johnson 1987; Neale and Nader 1973; Pietrak and Wisniewski 2015).
17 Volume fraction of aggregates and size and porosity of the ITZ have contradicting effects on the
18 transport properties of concrete. In a statistical study on conductivity of concrete, Zhou and Li
19 (2010) showed that, the decreasing effect of aggregate volume fraction ratio can be completely
20 cancelled out by high conductivity of the ITZ.

21 In order to study water movement in concrete, multi-scaled modeling is well accepted (Maekawa et
22 al. 2009). In this approach, water movement in concrete is modeled using the so-called meso-scale
23 method, in which concrete is modeled as a three-phase composite material with aggregates
24 embedded in cement paste matrix and the interfacial transition zone (ITZ) on the interface between
25 the aggregates and the surrounding cement paste. Numerical meso-scale modeling of concrete

1 material allows detailed investigation of the effect of ITZ and aggregate size and distribution on the
2 water transport properties of concrete. This approach can be very computationally demanding.
3 However, with the significant advance in computer technology, this is now possible. Several meso-
4 scale numerical studies by means of either the Finite Element (FE) method (Li et al. 2017; Li et al.
5 2016; Zhou and Li 2010) or lattice-type network models based on Voronoi tessellation
6 (Dehghanpoor Abyaneh et al. 2013; Wang and Ueda 2011; Wang and Ueda 2013) have been
7 established to model the water ingress in concrete material at meso-scale level.

8 From the above discussion, it can be inferred that transport properties of concrete as a composite
9 material depends on volume fraction ratio of aggregates, transport properties of cement paste matrix
10 and size and transport properties of the ITZ, most of which, especially the properties of ITZ, are
11 highly variable (Winslow et al. 1994). Therefore, investigation of transport properties of concrete
12 requires a probabilistic approach. Although Zhou and Li (2010), using a two-dimensional FE
13 model, conducted a sensitivity analysis on the effect of ITZ properties on hydraulic conductivity of
14 concrete, their analysis was not probabilistic. In this paper, in order to study the effect of the above-
15 mentioned factors on conductivity of concrete, a three-dimensional FE analysis, at meso-scale level,
16 embedded in a probabilistic procedure is employed. The formulation of the FE model is presented
17 and the model is verified with available experimental results. Based on rational probability density
18 functions for the conductivity of mortar matrix and the ITZ, a probabilistic sensitivity analysis is
19 conducted. Finally, an expression quantifying effect of aggregated volume fraction ratio and
20 conductivity of mortar and ITZ on overall water conductivity of concrete is presented.

21 **RESEARCH SIGNIFICANCE**

22 As a major water transport property, which can be used as an indicator to assess durability of
23 concrete, hydraulic conductivity depends on highly variable hydraulic conductivity of its
24 constituents: mortar, aggregate and the ITZ. Despite many studies that have been carried out on the
25 influence of properties of concrete constituents on its conductivity, due to highly variable nature of

1 these properties, the published results are still not consistence. In order to investigate the extent of
2 effect of variability of concrete constituents on its hydraulic conductivity, a probabilistic analysis is
3 needed. It is in this regard that the present paper proposes a probabilistic methodology for
4 investigating relation of hydraulic conductivity of concrete to properties of its constituents.

5 **PRINCIPAL MECHANISM OF WATER FLOW IN CONCRETE**

6 Water flow in saturated porous media such as concrete can be mathematically described using
7 Darcy's law. Analogues to other simple linear transport laws in electricity (Ohm's law), diffusion
8 (Fick's law) and the heat transfer (Fourier's law), Darcy's law establishes a relationship between
9 flow and energy gradient, which is hydraulic potential in the case of water flow, through a transport
10 property referred to as the conductivity. A unified theoretical framework can be applied to heat,
11 diffusion and electrical current and water flow (Hall and Hoff 2011). Conduction can be defined as
12 a flow process of water through a saturated medium, here concrete, under a hydraulic gradient. The
13 validity of Darcy's law will mathematically be acknowledged as,

$$14 \quad q = -K\nabla h \quad (1)$$

15 where K is the conductivity coefficient, q is water flow, ∇ is the gradient operator and h is the
16 hydraulic potential. For steady state conduction, continuity requires that,

$$17 \quad \nabla q = 0 \quad (2)$$

18 Therefore, given that K is constant, Equations (1) and (2) reduce to,

$$19 \quad \nabla^2 h = 0 \quad (3)$$

20 where ∇^2 is the Laplace operator, and the resulted differential equation is the Laplace equation. By
21 having the boundary conditions, variation of hydraulic potential and flow can be determined. There
22 are two types of boundary conditions for the general water transport process, which can be
23 formulated as follows,

1 size distribution of aggregates is determined by given grading curve from sieve analysis. In the
2 numerical analysis of concrete at the meso-scale level, it is common to use an optimal gradation
3 initially proposed by the Fuller for the aggregate size distribution (Li et al. 2016; Ma et al. 2016;
4 Wang et al. 2015).

$$P(d) = 100 \left(\frac{d}{d_{\max}} \right)^{\gamma} \quad (6)$$

5
6 where d is the size of the aggregate, d_{\max} is the maximum size of aggregates and $P(d)$ is the
7 percentage of aggregates having a size smaller than d . γ is a constant varying from 0.45 to 0.70. In
8 this study, a value of 0.50 is used for the gradation curve. Furthermore, for simplicity, only coarse
9 aggregates larger than 3.00 mm (0.118 in) are modeled, and the maximum aggregate size is 20 mm
10 (0.787 in). The large number of fine aggregates together with the cement matrix is treated as mortar,
11 for which homogenous water transport properties, conductivity in this study, are used.

12 For random generation of aggregates, a standard procedure from the available literature (Ma et al.
13 2016; Wang et al. 2015) is devised. The basic idea is to generate and place aggregates in a repeated
14 manner and with no overlap and boundary wall collision, until the target volume fraction is
15 achieved. Spherical particles are used to model the coarse aggregates for convenience.

16 **Finite Element (FE) Model**

17 In order to solve the differential equation governing hydraulic conduction in concrete at meso-scale
18 level, shown in Equation (3), different methods such as the finite difference method or the FE can
19 be used. In the numerical methods that use the finite difference technique, discretization based on
20 lattice-type network is commonly employed (Dehghanpoor Abyaneh et al. 2013). The FE method,
21 which is based on meshing the body into small elements, has also successfully been employed for
22 solving the water transport (Li et al. 2017; Li et al. 2016) as well as mechanical (Wang et al. 2015;
23 Xu and Chen 2016) problems at meso-scale level. Furthermore, the FE method has also been used

1 in the macro-scale modeling of water movement in concrete (Rahal et al. 2016; Van Belleghem et
2 al. 2016; West and Holmes 2005).

3 Mesh generation of complex three-dimensional meso-scale models in presence of the ITZ, which is
4 extremely thin compared to the normal size of coarse aggregates, is still a challenging task. Xu and
5 Chen (2016) concluded that using solid elements for the ITZ requires very fine meshing and as such
6 it is computationally demanding. They suggested the interface element as an alternative for
7 modeling this zone. The zero-thickness interface element has been used by Li et al. (2016) for
8 modeling the ITZ. The interface element is inserted between the solid elements representing the
9 aggregates and the mortar matrix. When used in the transport problems, this element conducts water
10 between the aggregates and the mortar.

11 In this paper, using the commercially available FE program, ANSYS (2016), a different approach in
12 modeling the ITZ is followed. As **Fig. 1** shows, the ITZ is modeled using shell elements, and solid
13 element is used for modeling the mortar matrix. Furthermore, as conductivity of aggregates is
14 negligible (compared with that of mortar matrix) the aggregates are not modeled.

15 **Fig. 1**

16 Following the previous discussion of the analogy between governing equation in the heat transfer
17 and water transport problems, in this study, capabilities of ANSYS program in heat transfer are
18 used to model water flow concrete. A three-dimensional conductive element SOLID70 with three-
19 dimensional conduction, shown in **Fig. 2(a)** is used for modeling the mortar matrix. The element
20 has eight nodes (six nodes in case of tetrahedral element) with a single degree of freedom,
21 temperature, at each node.

22 **Fig. 2**

23 The element SHELL57 is a three-dimensional shell element capable of modeling in-plane
24 conduction, shown in **Fig. 2(b)**, is used to model conductivity of the ITZ. The element has four

1 nodes (or three nodes in case of triangular element) capable of having temperature degrees of
2 freedom, hydraulic potential in this study, at each node. As **Fig. 1** shows, using zero-flux boundary
3 condition, see Equation (4b), water flow normal to aggregate surface is set to zero.

4 The FE model proposed in this study eliminates the need for sophisticated meshing required in
5 cases of modelling the ITZ using three-dimensional solid element. By introducing the shell element
6 for modelling the ITZ, there is no need to use interface element, which adds extra nodes in the FE
7 model. The number of nodes required for modelling the ITZ using the interface element are twice
8 those required when shell element is used. Furthermore, by replacing the non-conductive aggregate
9 elements with appropriate flux boundary conditions, the number of solid element is considerably
10 reduced. The proposed FE method is robust and can be used for evaluation of hydraulic
11 conductivity of concrete with different aggregate volume fractions. Nonetheless, given the very fine
12 mesh required in cases with high aggregate volume fraction, the meshing process is still time
13 consuming and requires large storage space. Any improvement, which leads to reduction in
14 meshing time and increases the meshing quality, would enhance the proposed FE method.

15 **Validation**

16 In order to validate the FE model described in the previous section for the analysis of hydraulic
17 conductivity of concrete at meso-scale level, samples from Li et al. (2016) study are considered in
18 this section. The laboratory specimens have cylindrical shape with 61.8 μ (2.43 in) diameter and
19 40.0 mm (1.57 in) height. For coarse aggregate, non-conductive equal-sized spherical Glass
20 particles with 6 mm (0.236 in) and 12 mm (0.472 in) were used. Typical random aggregate
21 generation for specimens with 0.10 to 0.40 aggregate Volume Fraction Ratios (VFR), denoted as ϕ
22 in this paper, can be seen in **Fig. 3**. For the specimen with VFR = 0.5, number of particles with 6
23 mm (0.236 in) and 12 mm (0.472 in) size are 292 and 30, respectively. In order to generate the flow
24 gradient, hydraulic potentials of 1300 mm (51.18 in) and 0 mm (0 in) were applied to the top and
25 bottom surface of the cylindrical specimen, respectively.

1 **Fig. 3**

2 In the FE analysis, the aggregate configuration is kept the same with experimental specimens as
3 depicted in **Fig. 3**. The Glass particles are considered as voids with zero flux inside the mortar body
4 as is indicated in **Fig. 4**. The mortar body is meshed using tetrahedral solid elements with maximum
5 size of 2.5 mm (0.10 in). A sensitivity analysis on mesh size showed that using this size lead to
6 adequately accurate results. In the boundary of internal voids and the mortar triangular shell
7 elements representing the ITZ are used. In **Fig. 4**, meshed body with the applied boundary
8 conditions for specimen with VFR of 0.30 is shown. In the experimental program of Li et al.
9 (2016), the outer face of cylinder was sealed. Thus, on the cylinder wall, a zero flux boundary
10 condition is applied.

11 **Fig. 4**

12 Results of the experimental program by Li et al. (2016) showed that the mean hydraulic
13 conductivity of mortar, K_m , is 0.0195 mm/sec (7.67×10^{-4} in/sec). As there is no direct method for
14 measurement of ITZ thickness, t_i , and conductivity, K_i , Li et al. (2016) used sensitivity analysis to
15 find the appropriate properties of this zone. They suggested that a thickness of 20 μm (7.87×10^{-7} in)
16 and a mean conductivity equal to 10 times that of mortar be used. For consistency, in the current
17 study, these values are used for validation of the proposed FE model.

18 Comparison between FE results obtained in this study and those of experimental program, as shown
19 in **Fig. 5**, shows that there is good agreement between the numerical and test results. For each
20 specimen, five readings have been reported by Li et al. (2016). The numerical FE result in **Fig. 5** is
21 based on average of five random particle generations. For high VFR values, the agreement between
22 the numerical and experimental results seems to be less. This could be attributed to higher surface
23 area between aggregates and the mortar, and as such larger ITZ volume, for high volume fraction
24 ratios. As properties of the ITZ are highly variable, variability of the effective conductivity would
25 be more for specimens with higher VFR values. It also worth noting that, in their numerical

1 analysis, Li et al. (2016) also attributed the difference between numerical and experimental results
2 to the fact that the property of ITZ is determined by assumptions and the sensitive analyses not from
3 experimental measurement.

4 **Fig. 5**

5 There are various simplified analytical and empirical expressions for effect of inclusion (no ITZ
6 effect) on the effective hydraulic conductivity of porous media with random dispersion of spherical
7 particles. A comparison between results of these models, the FE analysis used in this study and the
8 experimental results is shown in **Table 1**. The VFR of inclusion in this table is denoted as ϕ . It
9 should be noted that, for the experimental results in **Table 1**, effect of ITZ properties is included.

10 **Table 1**

11
12 Comparison of the results in **Table 1** shows that the conceptual models (Bruggeman 1935; Jeffrey
13 1973; Neale and Nader 1973) predict the effective conductivity very well. Furthermore, by
14 comparing the result of FE with no ITZ with the experimental results (mean of five reported
15 readings shown in **Fig. 5**), it can be concluded that the effect of ITZ is more pronounced for high
16 VFR values.

17 It is also worth noting that considering the hydraulic conductivity of 0.0195 mm/sec for mortar, for
18 the aggregate volume fraction ratios of 0.4 and 0.5, the lower bound k_e/k_m ratios that are obtained by
19 ignoring hydraulic conductivity of the particles and the ITZ are 0.5 and 0.4, respectively (see Table
20 1). These values are higher than those of Li et al.'s (2016) tests. This suggests that the hydraulic
21 conductivity of mortar in the mixes prepared for higher particle volume fractions deviate from that
22 of mortar with no particle.

23 **PROBABILISTIC ANALYSIS**

24 Hydraulic conductivity of concrete is a function of geometry and conductivity of its three phases,
25 i.e., mortar, aggregates and the ITZ. As all of these properties are highly uncertain, hydraulic

1 conductivity of concrete should be treated as a random variable. VFR and size distribution of coarse
2 aggregates is random and varies from place to place depending on the homogeneity of the concrete
3 mix. In this study, conductivity of a volume body of concrete is of interest, for which the VFR is
4 fixed. Nonetheless, the coarse aggregates that follow a predefined size distribution, shown in
5 Equation (6), are placed randomly in the volume cell. Five different VFR values of 0.10, 0.20, 0.30,
6 0.40 and 0.50 are considered.

7 Hydraulic conductivity of mortar and the thickness and conductivity of the ITZ are treated as
8 random variables. As the conductivity of adequately large volume cell is independent of its size, in
9 this study, the same concrete cylinder used in the verification section [from Li et al. (2016)] is
10 considered in the probabilistic analysis. The element used in the FE analysis and the mesh size is
11 also similar to that discussed in the verification section. For mortar conductivity, the mean and
12 coefficient of variation (COV) obtained by Li et al. (2016) are used, and it is assumed that this
13 variable follows the lognormal distribution. Statistical measurements for properties of the ITZ are
14 rare in the current literature. Only range of the ITZ size has been reported (Nemati and Gardoni
15 2005; Ollivier et al. 1995). On the other hand, there is little information about the statistical
16 distribution of the hydraulic conductivity of the ITZ (Bentz and Garboczi 1991; Wang et al. 2015).
17 In the absence of probabilistic models for the size and conductivity of the ITZ, the Uniform
18 distribution with the ranges available from the current literature can be used for modeling these
19 variables, as shown in **Table 2**. In the absence of information about frequency distribution of a
20 random variable, the Uniform distribution is a logical choice (Benjamin and Cornell 1975). Of
21 course, availability of more reliable probabilistic model will be a boost to the methodology
22 proposed in this study.

23 **Table 2**

24 Given the statistics for each random variable, the Monte Carlo technique is employed to find the
25 cumulative density function of the hydraulic conductivity of concrete as the independent response.

1 Trial simulations were conducted by Monte Carlo technique so that the effect of the sample size on
2 the results could be investigated. For this purpose, various sample sizes ranging between 100 and
3 1,500 for randomly generated values of the basic random variables were used. **Fig. 6** shows the
4 mean effective concrete conductivity (normalized with respect to conductivity of the mortar)
5 obtained with various sample sizes for the case with VFR of 0.40.

6 **Fig. 6**

7 As can be seen from **Fig. 6**, the mean response become stable when the sample size is 1000 and do
8 not change significantly for larger sample sizes. Thus, statistical assessment was performed for the
9 sample size of 1000 for the remaining part of the study. Furthermore, for each VFR, five samples
10 with different random aggregate distributions are used.

11 **RESULTS AND DISCUSSION**

12 Having the geometry, aggregate size distribution and material properties, the hydraulic conductivity
13 of concrete composite can be predicted by means of FE analysis according to Equation (5). As the
14 main variables are random in nature, the conductivity of concrete is probabilistic and its
15 distributions can be simulated by means of the Monte Carlo technique. Statistical measures of
16 concrete conductivity are investigated in this section. The Monte Carlo technique will also be used
17 to conduct sensitivity analysis and derive a relationship between the concrete conductivity and the
18 main random variables, i.e., hydraulic conductivity of mortar and properties of the ITZ.

19 **Uncertainty in hydraulic conductivity of concrete**

20 A typical result of simulated K_e/K_m ratios, based on one the randomly distributed aggregate cases, is
21 shown in **Fig. 7**. As is expected, by increasing the VFR, the K_e/K_m ratio decreases. It is clear that the
22 scatter of the K_e/K_m ratio increases with increasing aggregate VFR, and the range of the simulate
23 K_e/K_m ratio becomes wider. This can be attributed to increasing effect of ITZ properties, which have
24 more variability than that of conductivity of mortar. For higher VFR, the aggregate surface

1 available for the formation of ITZ is bigger, and as such, contribution of this zone in the final
2 conductivity would be higher. As the results of **Fig. 7** show, the coefficient of variation (COV), is
3 nearly proportional to the aggregate volume fraction ratio. It is worth noting that for consistency,
4 the same bin number has been used in plotting the histogram of K_e/K_m ratio for each of the VFR in
5 **Fig. 7**.

6 **Fig. 7**

7 For other cases of randomly distributed aggregates, similar results are obtained. In **Table 3**, for the
8 volume fraction ratio of 0.40, statistics of K_e/K_m ratio for all the considered cases (cases 1-5) are
9 shown. As it can be seen, for all of these cases, same trend of statistics is observed indicating that
10 the statistical measures obtained from each of these cases are consistent. This shows that the
11 random position of aggregates does not have considerable effect on statistics of the concrete
12 conductivity. Therefore, for the next subsections, results of simulation for all of the considered
13 cases (for each VFR) are combined together, i.e., for each VFR, 5000 samples are used.

14 **Table 3**

15 The minimum and maximum values in **Table 3** correspond to the lower and upper bound values of
16 the ITZ properties shown in **Table 2**. If the model proposed by Neale and Nader (1973) is used for
17 predicting the effective hydraulic conductivity of concrete, a value of 0.50 is obtained for the K_e/K_m
18 ratio (see **Table 1**). This is consistent with the minimum value shown in **Table 3**. By comparing the
19 maximum and minimum values, it is interesting to note that inclusion of the ITZ properties could
20 results in an effective hydraulic conductivity three times that of without the inclusion. In the
21 subsequent sections, this will be investigated in more details.

22 **Sensitivity analysis**

23 In order to find the most important random variables affecting conductivity of concrete, that are the
24 hydraulic conductivity of mortar and conductivity and thickness of the ITZ, a probabilistic

1 sensitivity analysis based on Pearson's correlation coefficient, was conducted. In the probabilistic
2 sensitivities (based on sample simulated by the Monte Carlo technique), any interaction among the
3 input random variables will be correctly reflected in the probabilistic sensitivities. The bar chart in
4 **Fig. 8** presents the main random variables, as well as the correlation coefficients associated with
5 each of these random variables. It is worth noting the simulated values of all the five cases are
6 combined in the results shown in **Fig. 8**. This means that a total number of 5000 samples are used in
7 derivation of each correlation coefficient.

8 **Fig. 8**

9 Results of the sensitivity analysis shown in **Fig. 8** clearly indicate that sensitivity coefficients,
10 represented by Pearson's correlation coefficient, ρ , vary with the aggregate VFR. For low VFR, the
11 ITZ properties, i.e., the hydraulic conductivity K_i and thickness, t_i , do not have big effect, while for
12 high aggregate VFR, the effect of these properties is considerable. Correlation of effective hydraulic
13 conductivity, K_e , with conductivity and thickness of the ITZ is the same. This is natural, as passage
14 of water through this zone can be logically resembled as movement of water within a water channel,
15 in which thickness of ITZ represents the channel width and ITZ conductivity represents the water
16 speed. The total quantity of water passing through the channel would be proportional to the product
17 of these quantities. Therefore, the unified term $K_i \times t_i$ can be used to relate ITZ properties to
18 conductivity of concrete as a composite material. For the reference, correlation of effective
19 hydraulic conductivity of concrete to this term is added in **Fig. 8**. There is high correlation between
20 this product term and the concrete conductivity. It can be concluded that except for the aggregate
21 volume fraction of 0.10, for all other cases, the term $K_i \times t_i$ has a dominant impact on the concrete
22 conductivity. This highlights the importance of the ITZ and its effect on the overall hydraulic
23 conductivity of concrete as a composite material.

1 **Model fitting**

2 According to Neale and Nader (1973), using a rational function, effective hydraulic conductivity of
3 composite material with randomly dispersed spherical dispersion can be related to volume fraction
4 ratio of inclusion, here the aggregate VFR (see **Table 1**). For low VFR (up to 0.50), with adequate
5 accuracy, this relationship can be linearized as follows,

$$\frac{K_e}{K_m} = 1 - \alpha\varphi \quad (7)$$

6
7 The parameter α is a reduction factor, which accounts for effect of aggregate VFR. This relationship
8 does not account for the effect of ITZ properties. Results of the sensitivity factors in the previous
9 section showed that properties of the ITZ represented by the product term $K_i \times t_i$ have the biggest
10 impact on the effective hydraulic conductivity of concrete, K_e . Normalizing the effective hydraulic
11 conductivity, K_e , with respect to hydraulic conductivity of mortar, K_m , results in the $K_i \times t_i / K_m$ term.
12 If the original relationship between normalised conductivity, K_e/K_m , proposed by Neale and Nader
13 (1973) is used as a basis for a new relationship considering effect of ITZ properties, the following
14 general model can be advised,

$$\frac{K_e}{K_m} = 1 - \left(\alpha - \beta \frac{K_i t_i}{K_m d_{avg}} \right) \varphi \quad (8)$$

15
16 where α and β are the fitting parameters. The variable d_{avg} is the average size of aggregate that can
17 be easily determined using the aggregate size distribution. This variable is introduced to define a
18 new dimensionless quantity, $K_i \times t_i / (K_m \times D_{avg})$, which facilitate fitting of a new model relating the
19 normalized concrete conductivity, K_e/K_m , to two dimensionless quantities that are φ and $K_i \times t_i /$
20 $(K_m \times d_{avg})$. The general model shown in Equation 8 physically predicts consistent values for
21 extreme values of the dimensionless variables: as $\varphi \rightarrow 0$, $K_e/K_m \rightarrow 0$, and as $K_i \times t_i \rightarrow 0$, $K_e/K_m \rightarrow 1$
22 $- \alpha\varphi$. Considering the assumptions made for the aggregate size distribution in this study [$d_{min} = 3$
23 mm (0.118 in), $d_{max} = 20$ mm (0.787 in) and $\gamma = 0.50$ for Fuller curve], the average aggregate size
24 can be determined as follows,

$$d_{avg} = \int_{d_{min}}^{d_{max}} x \cdot f_D(x) dx \quad (9a)$$

$$d_{avg} = \int_{d_{min}}^{d_{max}} x \cdot \frac{\gamma}{d_{max}} x^{\gamma-1} dx = \frac{\gamma}{d_{max}} \int_{d_{min}}^{d_{max}} x^\gamma dx = \frac{\gamma}{\gamma+1} \left[1 - \left(\frac{d_{min}}{d_{max}} \right)^{\gamma+1} \right] d_{max} = 6.28 \text{ mm} (0.247 \text{ in}) \quad (9b)$$

1 where $f_D(x)$ is the probability density function of the aggregate size, which is determined by taking
 2 the first derivative of the aggregate distribution size function given in Equation (5). Fitting the
 3 results obtained from 5000 simulations to Equation (8) results in the following equation relating the
 4 normalized concrete conductivity to the two-abovementioned dimensionless parameters.

$$\frac{K_e}{K_m} = 1.0 - \left(1.1 - 3.0 \frac{K_i t_i}{K_m d_{avg}} \right) \varphi \quad (10)$$

5
 6 For convenience, the fitting parameters α and β are rounded. A comparison between results of
 7 simulation for concrete conductivity with those obtained from Equation (10) shows that the
 8 coefficient of determination, R^2 , is about 0.98. This shows that the proposed expression well
 9 predicts the concrete conductivity considering the most important variables affecting the concrete
 10 conductivity. In **Fig. 9**, the relationship between the independent dimensionless variables and the
 11 effective hydraulic conductivity, K_e/K_m , is graphically shown.

12 **Fig. 9**

13 Equation (10) can be used to find the critical ITZ properties that cancel out the adverse effect of
 14 aggregate VFR. According to this equation, two extreme values lead to a $K_e/K_m = 1.0$. The first
 15 solution is $\varphi = 1.0$, which is a trivial solution. The other solution relates the critical properties of
 16 ITZ to properties of matrix (mortar here) and size distribution of aggregates represented by d_{avg} . It
 17 shows that when the product $K_i \times t_i$ exceeds $0.367(K_m \times d_{avg})$, the adverse effect of aggregate volume
 18 fraction on concrete conductivity is cancelled out. In **Fig. 9**, these two solutions are shown. It is
 19 worth noting that if the values used in the model verification are substituted to find the $K_i \times t_i /$
 20 $(K_m \times d_{avg})$ ratio, a value of 0.032 results, which is considerably lower than the critical value, i.e.,

1 0.367. On the other hand, using the extreme value shown in **Table 2** for the ITZ properties [$K_i/K_m =$
2 50 and $t_i = 0.10$ mm (0.0039 in)] results in 0.796 for this ratio. The available information about
3 properties of the ITZ is limited to make a solid conclusion on whether this critical ratio is met or
4 not. Nonetheless, the proposed expression in Equation (10) shows the significance of the ITZ and
5 its effect on conductivity of concrete as a composite material. More research on identification of
6 properties of ITZ using experimental data is required.

7 **CONCLUSION**

8 In this paper, with the aid of the Monte Carlo technique, a probabilistic study on variability of the
9 hydraulic conductivity of concrete and its relation to conductivity of concrete constituents, i.e.,
10 aggregate, mortar and the ITZ, at the meso-scale level is conducted. Within this probabilistic
11 procedure, a numerical analysis using the FE method, which was verified using experimental
12 results, is proposed. The proposed numerical model takes advantage of analogy between heat
13 transfer and water flow. It was shown that the properties of the ITZ, i.e., its thickness and hydraulic
14 conductivity have high correlation with the hydraulic conductivity of concrete. By taking advantage
15 of some of the available analytical models relating conductivity of composite material to volume
16 fraction of non-conductive particles, a new conceptual model relating effective hydraulic
17 conductivity of concrete to aggregate volume fraction, thickness of the ITZ and hydraulic
18 conductivities of mortar and the ITZ is proposed. Comparing the results predicted based on this
19 model and those obtained from the FE method, showed that this model can predict hydraulic
20 conductivity of concrete with very good accuracy. The model can be a useful tool for further
21 parametric studies on the role of the ITZ and mortar properties on overall conductivity of concrete
22 as a composite material.

23 **ACKNOWLEDGEMENT**

24 Financial support from Metro Trains Melbourne, Australia and Australian Research Council under
25 DP140101547, LP150100413 and DP170102211 grants is gratefully acknowledged.

REFERENCES

- 1
- 2 ANSYS. 2016. ANSYS Reference Manual, Swanson Analysis Systems, Houston, PA.
- 3 Benjamin, J., and Cornell, C. (1975). *Probability, statistics and decision for civil engineers*,
- 4 McGraw-Hill, New York, United States.
- 5 Bentz, D. P., and Garboczi, E. J. (1991). "Simulation Studies of the Effects of Mineral
- 6 Admixtures on the Cement Paste-Aggregate Interfacial Zone." *ACI Materials Journal*,
- 7 88(8), 518-529.
- 8 Breton, D., Ollivier, J. P., and Ballivy, G. (1992). "Diffusivity of chloride ions in the
- 9 transition zone between cement paste and granite." *Proceeding of the RILEM*
- 10 *International Conference, Interfaces in Cementitious Composites*.
- 11 Bruggeman, D. (1935). "Dielectric constant and conductivity of mixtures of isotropic
- 12 materials." *Ann Phys (Leipzig)*, 24, 636-679.
- 13 Dehghanpoor Abyaneh, S., Wong, H. S., and Buenfeld, N. R. (2013). "Modelling the
- 14 diffusivity of mortar and concrete using a three-dimensional mesostructure with several
- 15 aggregate shapes." *Computational Materials Science*, 78, 63-73.
- 16 Garboczi, E. J., and Bentz, D. P. (1996). "Modelling of the microstructure and transport
- 17 properties of concrete." *Construction and Building Materials*, 10(5), 293-300.
- 18 Halamickova, P., Detwiler, R. J., Bentz, D. P., and Garboczi, E. J. (1995). "Water
- 19 permeability and chloride ion diffusion in portland cement mortars: Relationship to sand
- 20 content and critical pore diameter." *Cement and Concrete Research*, 25(4), 790-802.
- 21 Hall, C. (1994). "Barrier performance of concrete: a review of fluid transport theory."
- 22 *Materials and Structures*, 27(5), 291-306.

- 1 Hall, C., and Hoff, W. D. (2011). *Water transport in brick, stone and concrete*, CRC Press.
- 2 Hall, C., Hoff, W. D., and Wilson, M. A. (1993). "Effect of non-sorptive inclusions on
3 capillary absorption by a porous material." *Journal of Physics D: Applied Physics*, 26(1),
4 31.
- 5 Hasselman, D., and Johnson, L. F. (1987). "Effective thermal conductivity of composites with
6 interfacial thermal barrier resistance." *Journal of Composite Materials*, 21(6), 508-515.
- 7 Ho, D. W. S., and Chirgwin, G. J. (1996). "A performance specification for durable concrete."
8 *Construction and Building Materials*, 10(5), 375-379.
- 9 ITA Working Group on Maintenance (1991). "Report on the damaging effects of water on
10 tunnels during their working life." *Tunnelling and Underground Space Technology*, 6(1),
11 11-76.
- 12 Jeffrey, D. J. (1973). "Conduction through a random suspension of spheres." *Proceedings of*
13 *the Royal Society of London A: Mathematical, Physical and Engineering Sciences*, The
14 Royal Society, 355-367.
- 15 Leech, C., Lockington, D., and Dux, P. (2003). "Unsaturated diffusivity functions for concrete
16 derived from NMR images." *Materials and Structures*, 36(6), 413-418.
- 17 Li, C.Q., Lawanwisut, W., Zheng, J.J. and Kijawatworawet, W. (2005), "Crack Width due to
18 Corroded Bar in Reinforced Concrete Structures", *Journal of Material & Structural*
19 *Reliability*, **3**, (2), 87 – 94
- 20 Li, X., Chen, S., Xu, Q., and Xu, Y. (2017). "Modeling the three-dimensional unsaturated
21 water transport in concrete at the mesoscale." *Computers & Structures*, 190, 61-74.

- 1 Li, X., Xu, Q., and Chen, S. (2016). "An experimental and numerical study on water
2 permeability of concrete." *Construction and Building Materials*, 105, 503-510.
- 3 Lockington, D., Leech, C., Parlange, J., and Dux, P. (2002). "The Sorptivity Test and
4 Predicting Resistance to Water Absorption in Concrete." *Innovations and Developments In
5 Concrete Materials And Construction: Proceedings of the International Conference*,
6 Thomas Telford Limited, 315-324.
- 7 Ma, H., Xu, W., and Li, Y. (2016). "Random aggregate model for mesoscopic structures and
8 mechanical analysis of fully-graded concrete." *Computers & Structures*, 177, 103-113.
- 9 Maekawa, K., Ishida, T., and Kishi, T. (2009). *Multi-scale modeling of structural concrete*,
10 Taylor & Francis, London and New York.
- 11 Murata, J., Ogihara, Y., Koshikawa, S., and Itoh, Y. (2004). "Study on watertightness of
12 concrete." *ACI Materials Journal*, 101(2), 107-116.
- 13 Neale, G. H., and Nader, W. K. (1973). "Prediction of transport processes within porous
14 media: diffusive flow processes within an homogeneous swarm of spherical particles."
15 *AIChE Journal*, 19(1), 112-119.
- 16 Nemati, K. M., and Gardoni, P. (2005). "Microstructural and statistical evaluation of
17 interfacial zone percolation in concrete." *11th International Conference on Fracture
18 (ICF11)*, 191-197.
- 19 Ollivier, J., Maso, J., and Bourdette, B. (1995). "Interfacial transition zone in concrete."
20 *Advanced Cement Based Materials*, 2(1), 30-38.
- 21 Pietrak, K., and Wisniewski, T. S. (2015). "A review of models for effective thermal
22 conductivity of composite materials." *Journal of Power Technologies*, 95(1), 14.

- 1 Rahal, S., Sellier, A., and Casaux-Ginestet, G. (2016). "Finite element modelling of
2 permeability in brittle materials cracked in tension." *International Journal of Solids and*
3 *Structures*, 1-15.
- 4 Russell, H. A., and Gilmore, J. (1997). "Inspection policy and procedures for rail transit
5 tunnels and underground structures." Transportation Research Board, 104.
- 6 Scrivener, K. L., Crumbie, A. K., and Laugesen, P. (2004). "The interfacial transition zone
7 (ITZ) between cement paste and aggregate in concrete." *Interface Science*, 12(4), 411-421.
- 8 Shane, J. D., Mason, T. O., Jennings, H. M., Garboczi, E. J., and Bentz, D. P. (2000). "Effect
9 of the interfacial transition zone on the conductivity of Portland cement mortars." *Journal*
10 *of the American Ceramic Society*, 83(5), 1137-1144.
- 11 Van Belleghem, B., Montoya, R., Dewanckele, J., Van den Steen, N., De Graeve, I.,
12 Deconinck, J., Cnudde, V., Van Tittelboom, K., and De Belie, N. (2016). "Capillary water
13 absorption in cracked and uncracked mortar – A comparison between experimental study
14 and finite element analysis." *Construction and Building Materials*, 110, 154-162.
- 15 Wang, L., and Ueda, T. (2011). "Mesoscale modeling of water penetration into concrete by
16 capillary absorption." *Ocean Engineering*, 38(4), 519-528.
- 17 Wang, L., and Ueda, T. (2013). "Mesoscale Modeling of Chloride Penetration in Unsaturated
18 Concrete Damaged by Freeze-Thaw Cycling." *Journal of Materials in Civil Engineering*,
19 26(5), 955-965.
- 20 Wang, X. F., Yang, Z. J., Yates, J. R., Jivkov, A. P., and Zhang, C. (2015). "Monte Carlo
21 simulations of mesoscale fracture modelling of concrete with random aggregates and
22 pores." *Construction and Building Materials*, 75, 35-45.

- 1 West, R. P., and Holmes, N. (2005). "Predicting moisture movement during the drying of
2 concrete floors using finite elements." *Construction and Building Materials*, 19(9), 674-
3 681.
- 4 Winslow, D. N., Cohen, M. D., Bentz, D. P., Snyder, K. A., and Garboczi, E. J. (1994).
5 "Percolation and pore structure in mortars and concrete." *Cement and concrete research*,
6 24(1), 25-37.
- 7 Wriggers, P., and Moftah, S. O. (2006). "Mesoscale models for concrete: Homogenisation and
8 damage behaviour." *Finite Elements in Analysis and Design*, 42(7), 623-636.
- 9 Wu, K., Shi, H., Xu, L., Ye, G., and De Schutter, G. (2016). "Microstructural characterization
10 of ITZ in blended cement concretes and its relation to transport properties." *Cement and
11 Concrete Research*, 79, 243-256.
- 12 Xu, Y., and Chen, S. (2016). "A method for modeling the damage behavior of concrete with a
13 three-phase mesostructure." *Construction and Building Materials*, 102, Part 1, 26-38.
- 14 Young, J. F., and Hansen, W. (1987). "Volume Relationships for C-S-H Formation Based on
15 Hydration Stoichiometries." *Materials Research Society Symposium Proceedings*, 85, 313-
16 322.
- 17 Zheng, J.J., Li, C.Q., and Zhou, X.Z. (2005), "Characterization of the Microstructure of
18 Interfacial Transition Zone in Concrete", *ACI Materials Journal*, **102**, (4), 265 – 271.
- 19 Zhou, C., and Li, K. (2010). "Numerical and statistical analysis of permeability of concrete as
20 a random heterogeneous composite." *Computers & Concrete*, 7(5), 469-482.

21

22

1

2

3

1 **TABLES AND FIGURES**

2 **List of Tables:**

3 **Table 1** – Results of K_e/K_m ratio with no ITZ (except test results)

4 **Table 2** – Statistical models for the basic random variables

5 **Table 3** – Statistics of the hydraulic conductivity of concrete expressed as K_e/K_m ratio ($\phi = 0.40$)

6

7 **List of Figures:**

8 **Fig. 1** – FE modeling of the ITZ

9 **Fig. 2** – Finite elements used in the numerical analysis (ANSYS 2016)

10 **Fig. 3** – Typical samples with aggregate different volume fraction ratios

11 **Fig. 4** – FE mesh and boundary conditions

12 **Fig. 5** – FE versus experimental results from Li et al. (2016)

13 **Fig. 6** – Effect of sample size on concrete effective conductivity ($\phi = 0.40$)

14 **Fig. 7** – Typical probability density functions of concrete conductivity

15 **Fig. 8** – Sensitivity of the hydraulic conductivity of concrete to the basic random variables

16 **Fig. 9** – Simulation versus predicted hydraulic conductivity of concrete

17

18

19

20

21

22

Table 1–Results of K_c/K_m ratio with no ITZ (except test results)

No.	VFR	Test	Neale and Nader (1973)		Jeffery (1973)	Bruggeman (1935)
			FE	$\frac{2(1-\varphi)}{2+\varphi}$	$1-1.5\varphi+0.588\varphi^2$	$(1-\varphi)^{3/2}$
1	0.1	0.93	0.83	0.86	0.86	0.85
2	0.2	0.75	0.71	0.73	0.72	0.72
3	0.3	0.70	0.60	0.61	0.60	0.59
4	0.4	0.32	0.51	0.50	0.49	0.46
5	0.5	0.18	0.42	0.40	0.40	0.35

Table 2–Statistical models for the basic random variables

Var.	Parameters	Distribution
K_m	Mean = 0.0195 mm/sec (7.67×10^{-4} in/sec), COV = 0.15	Lognormal
K_i	Min = 0, Max = 50×0.0195 mm/sec ($50 \times 7.67 \times 10^{-4}$ in/sec)	Uniform
t_i	Min = 0 , Max = 100 μm (0.0039 in)	Uniform

Table 3–Statistics of the hydraulic conductivity of concrete expressed as K_e/K_m ratio ($\phi = 0.40$)

Case	Min	Max	Mean	SD ¹	COV ²
1	0.51	1.47	0.81	0.234	0.288
2	0.51	1.64	0.82	0.235	0.287
3	0.52	1.44	0.82	0.223	0.273
4	0.52	1.51	0.82	0.219	0.268
5	0.51	1.58	0.83	0.240	0.290
All	0.51	1.64	0.82	0.230	0.280

¹SD = Standard Deviation

²COV = Coefficient of Variation

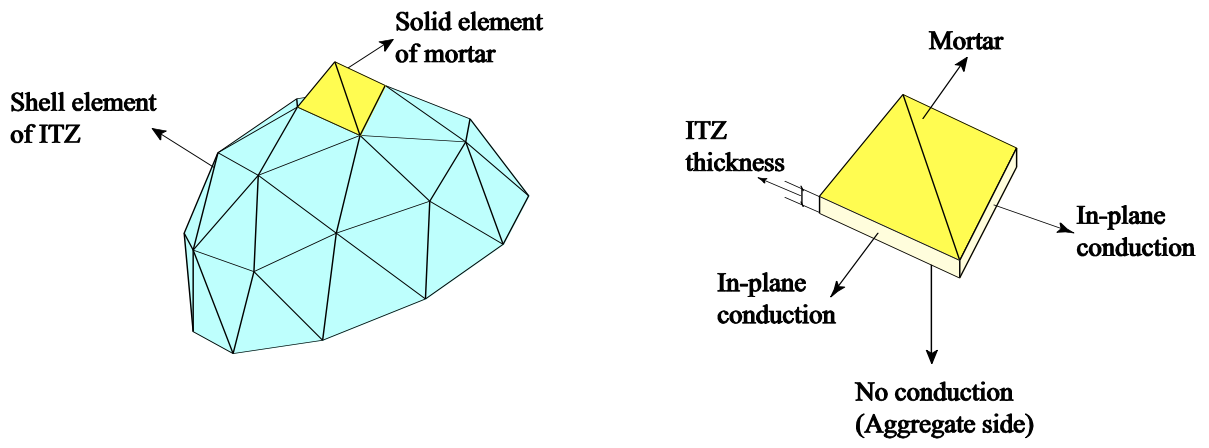


Fig. 1–FE modeling of the ITZ

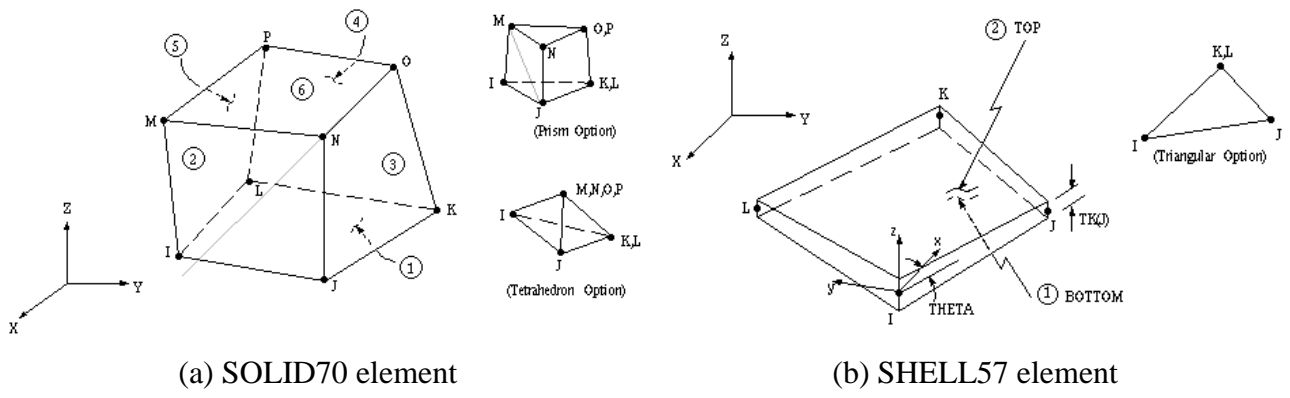
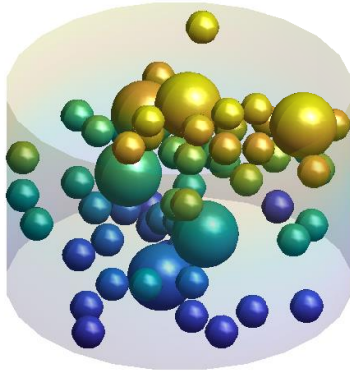
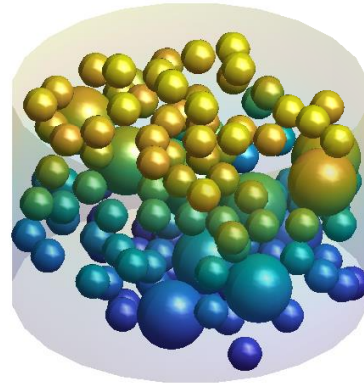


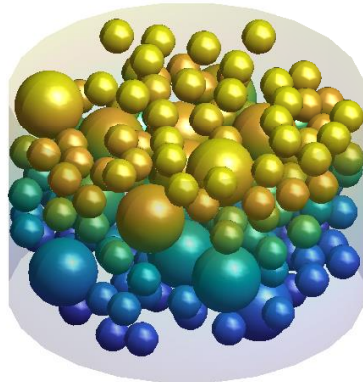
Fig. 2–Finite elements used in the numerical analysis (ANSYS 2016)



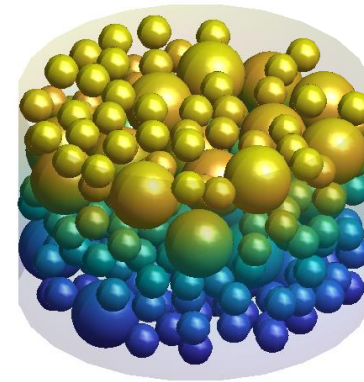
Number of 6 mm (0.236 in) = 58
 Number of 12 mm (0.471 in) size = 6
 (a) $\varphi = 0.10$



Number of 6 mm (0.236 in) = 117
 Number of 12 mm (0.471 in) size = 12
 (b) $\varphi = 0.20$



Number of 6 mm (0.236 in) = 175
 Number of 12 mm (0.471 in) size = 18
 (c) $\varphi = 0.50$



Number of 6 mm (0.236 in) = 234
 Number of 12 mm (0.471 in) size = 24
 (d) $\varphi = 0.40$

Fig. 3–Typical samples with aggregate different volume fraction ratios

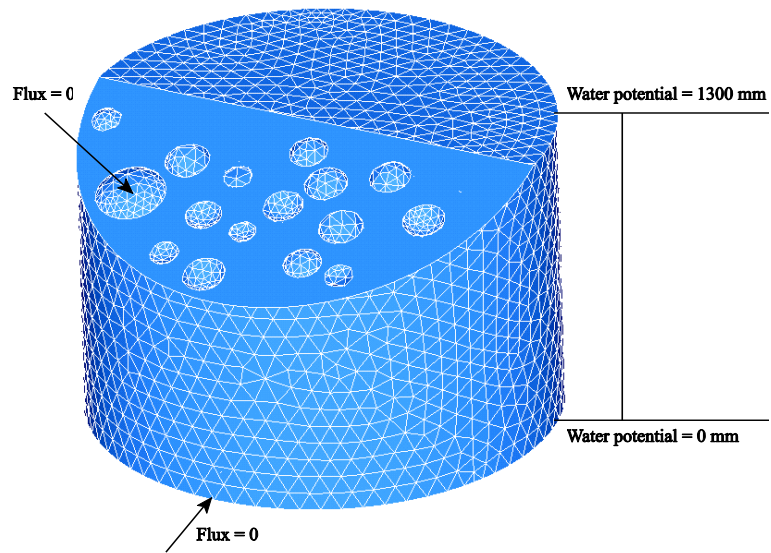


Fig. 4–FE mesh and boundary conditions

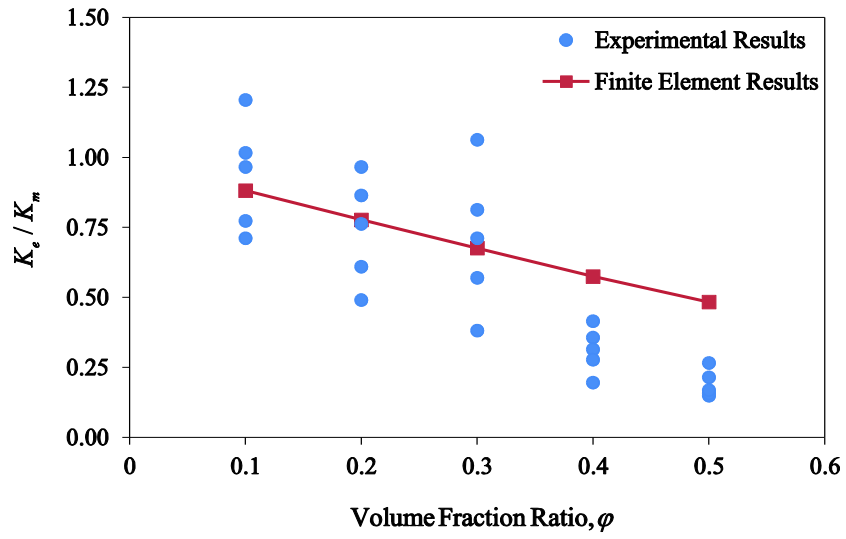


Fig. 5–FE versus experimental results from Li et al. (2016)

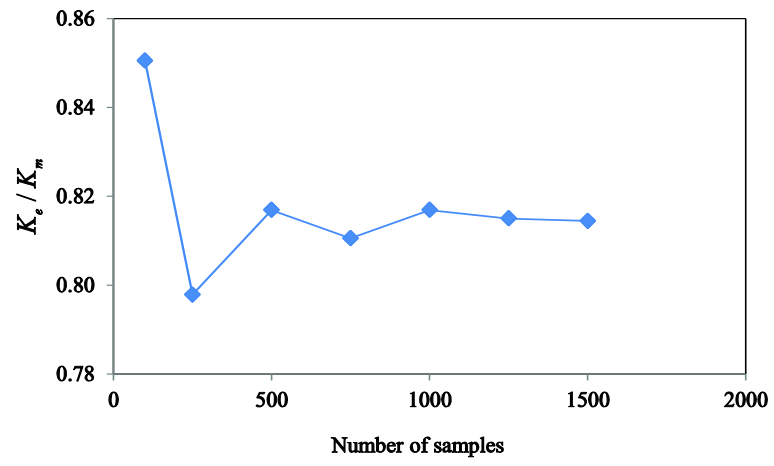


Fig. 6–Effect of sample size on concrete effective conductivity ($\phi = 0.40$)

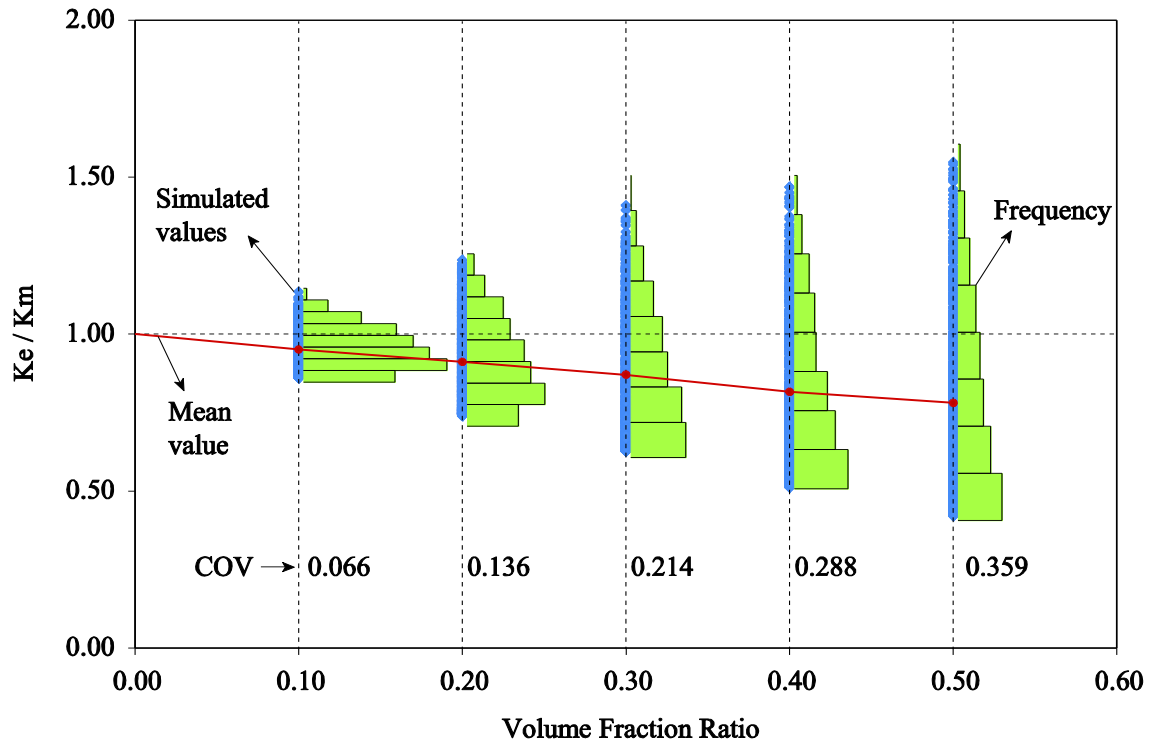


Fig. 7–Typical probability density functions of concrete conductivity

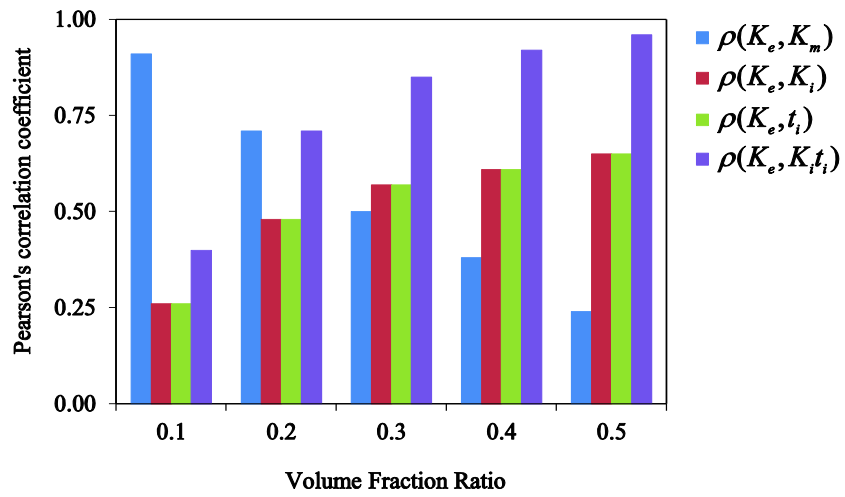


Fig. 8–Sensitivity of the hydraulic conductivity of concrete to the basic random variables

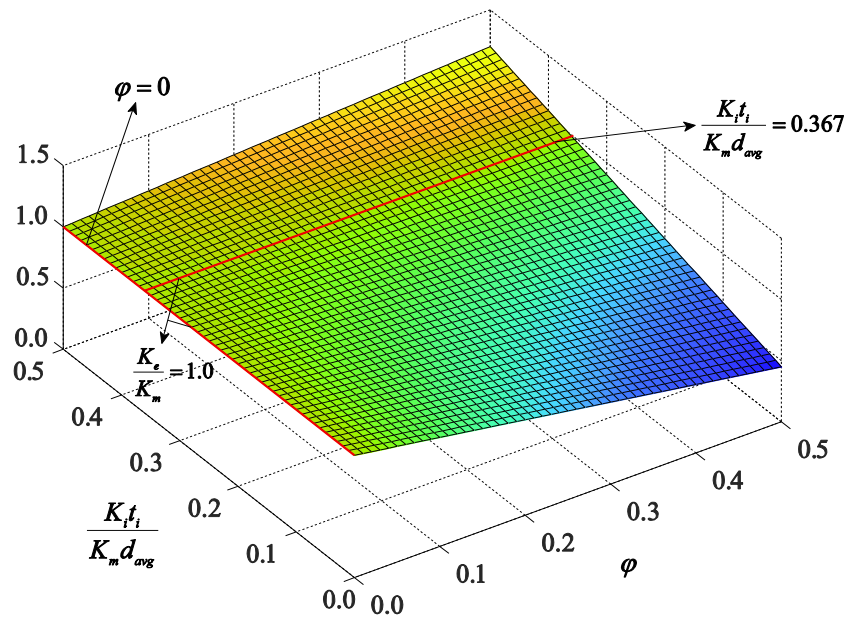


Fig. 9—Simulation versus predicted hydraulic conductivity of concrete